FRONTIERS OF PHYSICS

RESEARCH ARTICLE
Volume 18 / Issue 3 / 33303 / 2023

Theoretical investigation on optical properties of Möbius carbon nanobelts in one- and two-photon absorption

Zhiqiang Yang[1,2,*], Yichuan Chen[1,*], Jing Li[3,*], Chen Lu[4], Junfang Zhao[3], Mengtao Sun[1,†]

1 School of Mathematics and Physics, Beijing Advanced Innovation Center for Materials Genome Engineering, University of Science and Technology Beijing, Beijing 100083, China
2 Orient Scientific Software (Beijing) Technology Ltd, Beijing, China
3 Key Laboratory of Photochemical Conversion and Optoelectronic Materials, Technology Institution Physical and Chemistry, Chinese Academy of Sciences, Beijing 100190, China
4 College of Science, Liaoning Petrochemical University, Fushun 113001, China
Corresponding author. E-mail: †mengtaosun@ustb.edu.cn
*These authors contributed equally to this work.
Received October 19, 2022; accepted November 30, 2022

ABSTRACT

The first successful synthesis of fully fused and fully conjugated Möbius carbon nanobelts (CNBs) has attracted considerable attention. However, theoretical calculations based on such π-conjugated Möbius CNB are still insufficient. Herein, we theoretically investigated molecular spectroscopy of Möbius CNBs without and with n-butoxy groups via visualization methods. The results show that the presence of n-butoxy groups can significantly affect Möbius CNBs' optical performance, changing electron-hole coherence and enhancing two-photon absorption cross-sections. Our work provides a deeper understanding of photophysical mechanisms of Möbius CNBs in one- and two-photon absorption and reveals possible applications on optoelectronic devices.

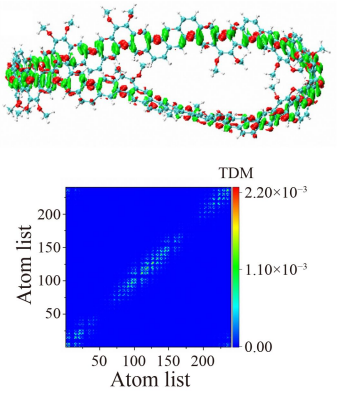

Keywords optical properties, Möbius carbon nanobelts, photon, spectroscopy

1 Introduction

The recent successful synthesis of large Möbius carbon nanobelts (CNBs) manifested as fully fused CNBs with twist by Segawa's group has attracted considerable attention [1], which certainly will promote the development of Möbius annular strips and bring great interest in Möbius molecules [2]. Since the concept of Möbius strip was born, its charm has been very touching and propagated in various figurative or abstract disciplines. From the physicochemical point of view, the presence of twists in Möbius molecules can change the charge density distributions in frontier molecular orbitals, affecting electron-spin interactions of different orbitals, thereby significantly impacting on their electronic, optical, and magnetic properties [3–6]. Moreover, topological characteristic in Möbius CNBs due to the structural twist with multiple conjugate rings further endows them with unique chiral properties, making them not only excellent candidates for fundamental researches on chirality, but also the ideal for constructing novel chiral materials [7, 8]. So far, a variety of Möbius molecules with fantastic topological structures have been designed and synthesized [9–15]. Two important milestones were the first synthesis of non-

Higher Education Press

https://doi.org/10.1007/s11467-022-1237-3

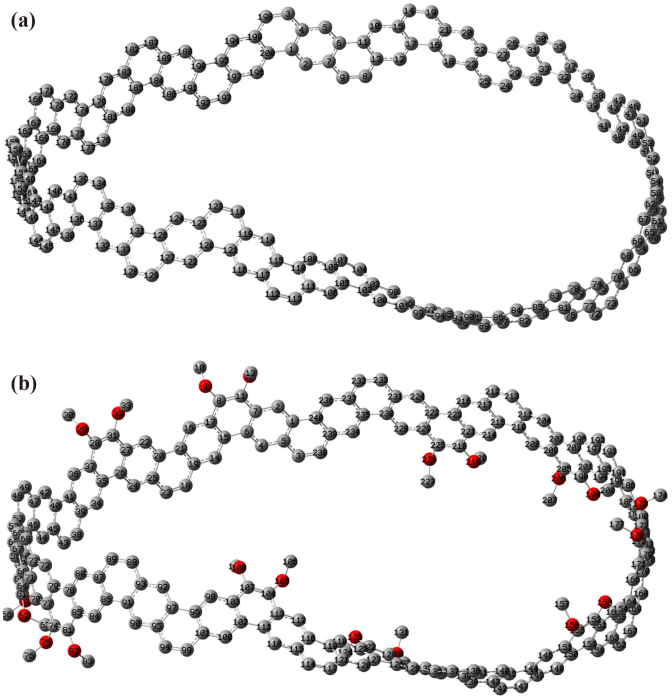

Fig. 1 The atomic list of Möbius CNBs without and with n-butoxy groups, where H atoms are not shown. **(a)** Möbius CNBs without n-butoxy groups, **(b)** Möbius CNBs with n-butoxy groups.

conjugated molecular Möbius double-stranded strip by Walba *et al.* [16] in 1982 and the synthesis and isolation of the first π-conjugated Möbius ring by Herges *et al.* [4] in 2003. The intriguing aspect of the recently synthesized Möbius CNB by Segawa's group is that the controllable extension of CNB with irreducible inner and outer faces to aromatic molecule with topological Möbius nanobelt, the simplest example of a carbolic non-orientable surface [1], which facilitates the theoretical calculations and qualitative investigations of Möbius molecules' physical mechanisms.

Möbius CNBs with fully conjugated and rigid carbon backbones have potential molecular optoelectronic applications [17, 18]. Organic molecules with conjugated structures are more prone to polarization under light irradiation, resulting in large carrier mobilities and greater absorbance and photoluminescence [19, 20]. Their optical sensitivity, efficient light harvesting and broad-spectrum absorption satisfy the applications of optoelectronic devices, such as sensors and solar cells. Furthermore, compared with one-photon absorption (OPA), Möbius CNBs are capable of excellent nonlinear performance due to large π-conjugated rings, such as great two-photon absorption (TPA) properties. Although the outstanding photophysical properties of Möbius CNBs have been demonstrated [1, 18], more detailed physical mechanisms are not well understood, such as the photoinduced delocalization characteristic in

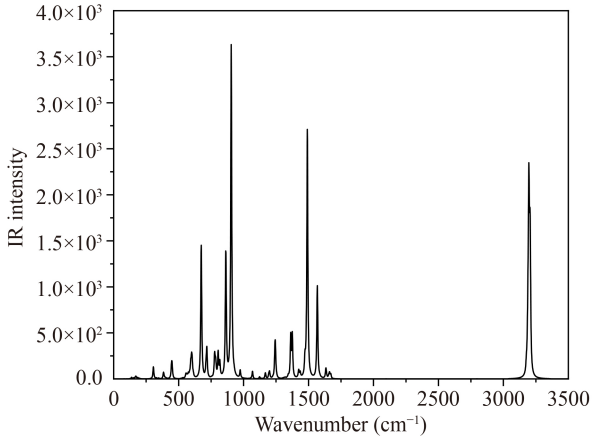

Fig. 2 IR absorption of Möbius CNBs without n-butoxy groups.

OPA and TPA and the influence of modification of n-butoxy groups on molecular photophysical performance. Therefore, the molecular spectroscopy investigations of Möbius CNBs are crucial.

In this paper, we theoretically investigated the molecular spectroscopy of Möbius CNBs without and with n-butoxy groups, and analyzed the electron-hole coherence of optical excitation process in different conditions through visualization methods. The results show that Möbius CNBs without and with n-butoxy groups all exhibit excellent optical properties, and the presence of n-butoxy groups changes the optical properties of the excited states and significantly enhances the TPA cross-section. Our study provides a deeper understanding of physical mechanisms of Möbius CNBs in one- and two-photon absorption and reveals possible applications on optoelectronic devices.

2 Methods

Structures of Möbius CNBs without and with n-butoxy groups were optimized by density functional theory (DFT) [21], B3LYP functional, and 6–31 G(d) basis set [22, 23], without any symmetry assumptions, using Gaussian 16 software [24]. Harmonic vibration frequency calculation at the same level was performed to verify all stationary points as local minima (with no imaginary frequency), where the lowest frequency is 0.8733 cm^{-1}, see IR spectroscopy in Fig. 2. Absorption spectroscopy was calculated with time-dependent DFT (TDDFT) [25], at the level of CAM-B3LYP functional [26], and 6–31 G(d) basis set. The visualization of transition density matrix (TDM) and charge density difference (CDD) was done with Multiwfn program [27, 28].

According to simplified sum-over-state (SOS) approach, the TPA cross-section can be defined as [29]

$$\sigma_{tp} = \frac{4\pi^2 a_0^5 \alpha}{15c} \frac{\omega^2 g(\omega)}{\Gamma_f} \delta_{tp}, \quad (1)$$

where the c is the speed of light, Γ_f is the lifetime of the final state, a_0 is Bohr radius, α is the fine structure constant, ω is the energy of the incident light, and $g(\omega)$ expresses the spectral line profile, which is assumed to be a δ function. The transition probability δ_{tp} in Eq. (1) can be expressed as

$$\delta_{tp} = 8 \sum_{\substack{m \neq g \\ m \neq f}} \frac{|\langle g|\mu|m\rangle|^2 |\langle m|\mu|f\rangle|^2}{\left(E_m - \frac{E_f}{2}\right)^2 + {\Gamma_f}^2} (1 + 2\cos^2\theta) + 8 \frac{|\Delta\mu_{gf}|^2 |\langle g|\mu|f\rangle|^2}{\left(\frac{E_f}{2}\right)^2 + {\Gamma_f}^2} (1 + 2\cos^2\varphi), \quad (2)$$

where $|g\rangle$ represents the ground state, $|f\rangle$ denotes final state, and $|m\rangle$ stands for intermediate state; μ is the electrical dipole moment operators, E_m and E_f are the excited state and final state energy, and $\Delta\mu_{gf} = \langle f|\mu|f\rangle - \langle g|\mu|g\rangle$ is the difference between the excited states' permanent dipole moments and that of the ground state; θ and φ are the angle between the vectors $\langle g|\mu|m\rangle$ and $\langle m|\mu|f\rangle$ and between the vectors $\Delta\mu_{gf}$ and $\langle g|\mu|f\rangle$, respectively.

3 Results and discussion

Figure 3 is the absorption spectra of Möbius CNBs in one- and two-photon absorption, respectively, where the structures of Möbius CNBs are inserted in the figures. Figures 3(a) and (b) are the one-photon absorption spectra of Möbius CNBs without and with n-butoxy groups. It is found that there is little of difference on the spectral profiles influenced by n-butoxy groups. Their exciton binding energies [30] are 1.20 and 1.18 eV, which reveals that the side chain of Möbius CNBs can slightly decrease the exciton binding energy. Generally, there is an essential difference between OPA and TPA, since TPA follows the nonlinear susceptibility relationship. It can be seen from Fig. 3(c) that S_{16} state is the strongest in TPA, while S_{19} is the strongest in OPA. According to SOS expression, the magnitude of transition dipole moment $|\langle g|\mu|f\rangle|^2$ contributes a "two-state term" process in TPA (green line), which is also the origin of the OPA oscillator strength, and S_{16} in TPA originates from $|\langle g|\mu|m\rangle|^2 |\langle m|\mu|f\rangle|^2$ (bule line), which is a "three-state

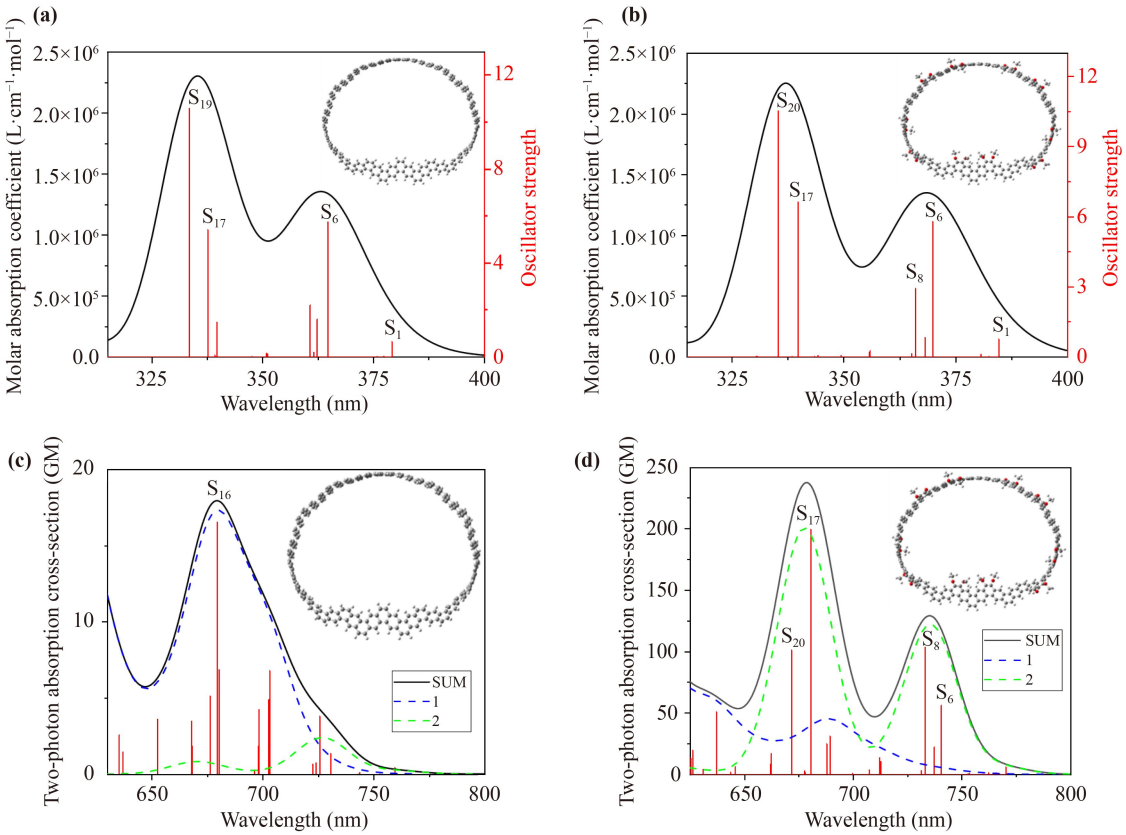

Fig. 3 One- and two-photon absorption spectra of Möbius CNBs with and without n-butoxy groups. **(a, b)** are one-photon absorption spectra, and **(c, d)** are two-photon absorption spectra. 1 and 2 stand for three-state term and two-state term, respectively.

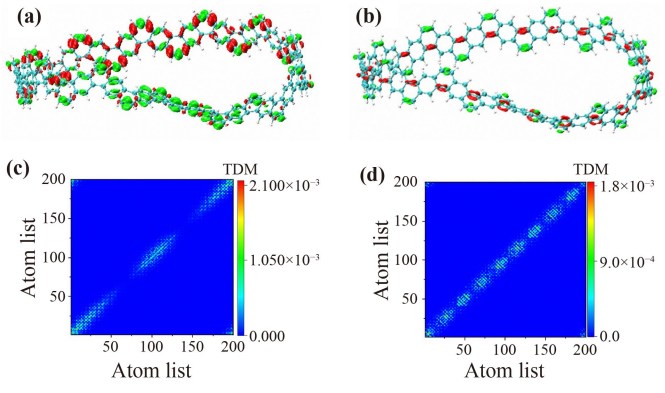

Fig. 4 CDD and TDM of Möbius CNBs without n-butoxy groups in OPA. **(a, b)** CDDs for S_6 and S_{19}, where the green and red stand for hole and electron, respectively; **(c, d)** TDMs for S_6 and S_{19}, respectively.

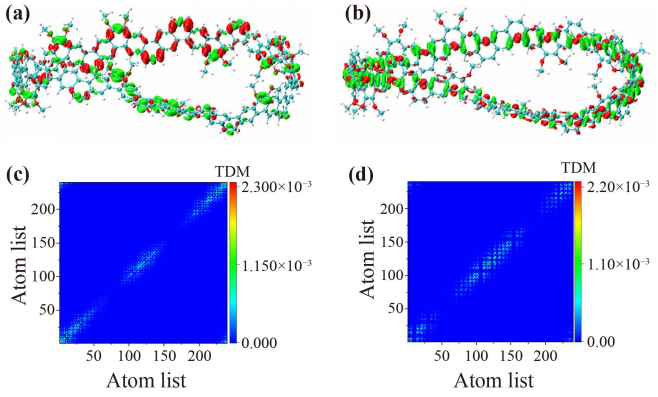

Fig. 5 CDD and TDM of Möbius CNBs with n-butoxy groups in OPA. **(a, b)** CDDs for S_6 and S_{20}, where the green and red stand for hole and electron, respectively; **(c, d)** TDMs for S_6 and S_{20}, respectively.

term" differentiated from the OPA. Besides, n-butoxy groups can significantly influence the spectral profiles in two-photon absorption, where TPA cross-section can be increased more than 10 times, see Figs. 3(c) and (d), because of different transition mechanism in TPA, which will be discussed later.

Figure 4 reveals the electron–hole distribution and electron–hole coherence [31] on two important electronic transitions (S_6 and S_{19}) in OPA in Möbius CNBs without n-butoxy groups, where atomic list can be seen from Fig. 1. CDD demonstrates that electron–holes are distributed within twist moiety and non-twist moiety in Möbius CNBs for S_6 in OPA, see Fig. 4(a); while for S_{19}, electron–holes are equally distributed within twist moiety and non-twist moiety of Möbius CNBs, see Fig. 4(b). TDM can further reveal the electrons separated from and holes can where to go. It is found that there are two nods in electron–hole distribution, which separate twist moiety and non-twist moiety in Möbius CNBs for S_6 in Fig. 4(c); while for S_{19}, electron–hole is equally distributed in twist moiety and non-twist moiety in Möbius CNBs, in which electron–hole coherence within 9 units equally is separated by 9 nods in Fig. 4(d). Thus, by CDD and TDM, optical physics of Möbius CNBs can be well understood.

For the Möbius CNBs with n-butoxy groups, Fig. 5 demonstrates that there are similar optical properties for the first absorption peak of S_6 electronic transition; while for the second strong peak at S_{20}, optical properties are similar with that of S_6 electronic transition, which reveals that the strain can still influence optical properties of this excited state. Thus, n-butoxy groups can convert of optical properties of Möbius CNBs. For two-photon absorption, the addition of n-butoxy groups can result in obvious effects on the nonlinear absorption properties and delocalization of excitation process. In TPA spectra, the first term "1" is two-step transitions via intermediate states in TPA, which is the main contribution for the transitions of Möbius CNBs without n-butoxy groups, see Fig. 3(c), and charge transfer distribution and electron–hole coherence in the first and second step transitions and each channel can be seen from Fig. 6(a). The second term "2" via direct transition from ground state to final state in TPA is the most important contribution for transitions of Möbius CNBs with n-butoxy groups, because of large difference between permanent dipole moments at ground and excited states, see Fig. 3(d); Moreover, first term "1" via two-step transitions is also contributed part of cross sections. So, the n-butoxy groups can significantly change the difference $\Delta\mu_{gf} = \langle f|\mu|f\rangle - \langle g|\mu|g\rangle$ between permanent dipole moments at ground and excited states, and increase of the TPA cross-section. The charge transfer distribution and electron–hole coherence in the one-step direct transitions for S_6 and S_{17} can be seen from Figs. 6(b) and (c).

Figure 7 demonstrates the Raman spectra of Möbius CNB and its twist and non-twist moieties. It can be found that the Raman spectra cannot identify the chirality of Möbius CNBs, even Möbius CNBs is divided into two separated parts of twist and non-twist moieties, respectively.

4 Conclusion

Molecular spectroscopy investigations of Möbius carbon nanobelts without and with n-butoxy groups reveal that Möbius CNBs are promising as emerging optoelectronic devices due to their efficient light harvesting and large TPA cross-sections. Electron–hole coherence analysis shows that compared with fully conjugated structures, Möbius CNBs with n-butoxy exhibit larger TPA cross-sections, and they are speculated to have better fluorescence efficiencies. In addition, Mobius CNBs are regarded as excellent chiral molecules, and more applications are still

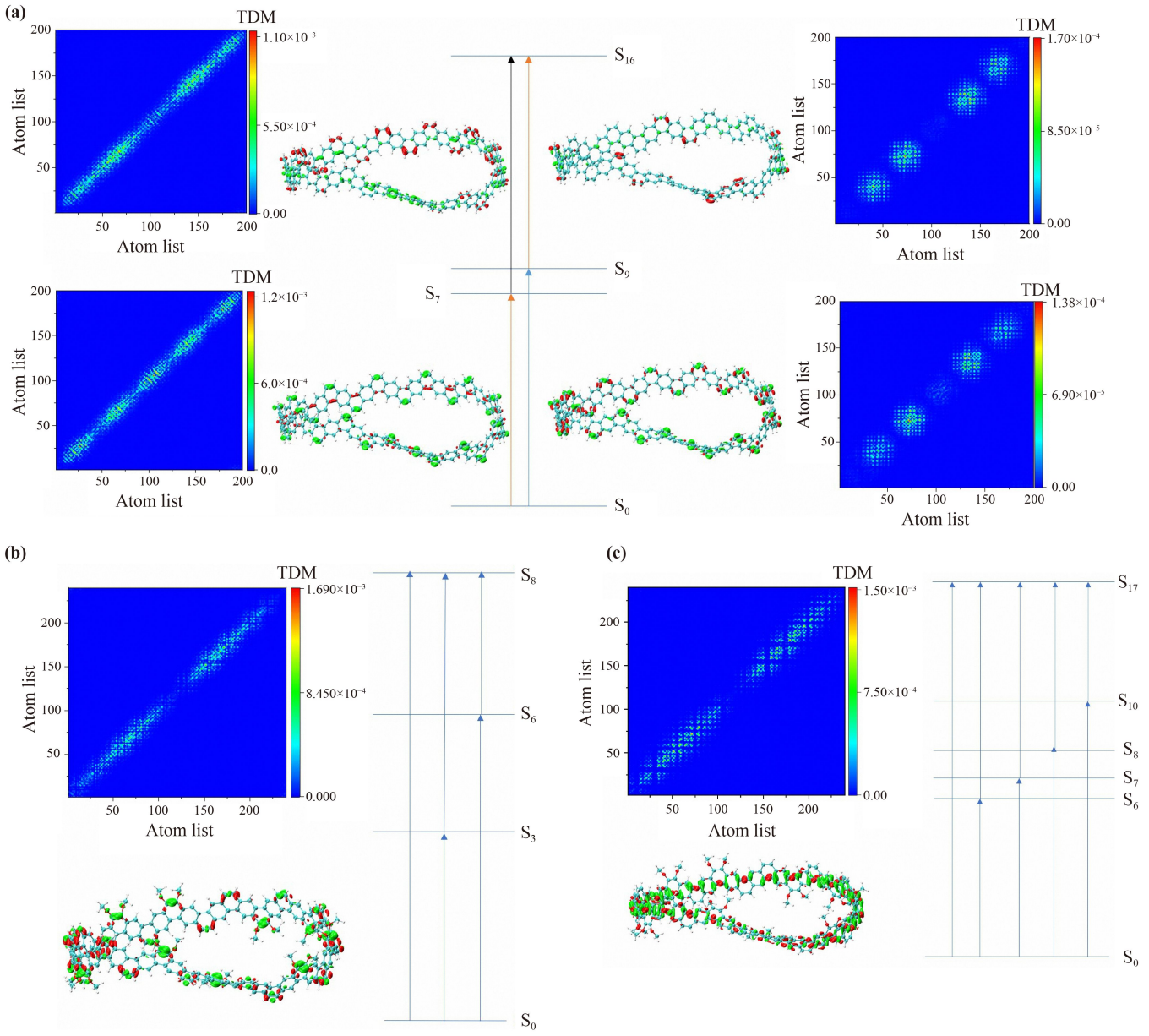

Fig. 6 Electronic transitions of Möbius CNBs without and with n-butoxy groups in TPA. **(a)** Electronic transitions of Möbius CNBs without n-butoxy groups, and **(b, c)** with n-butoxy groups.

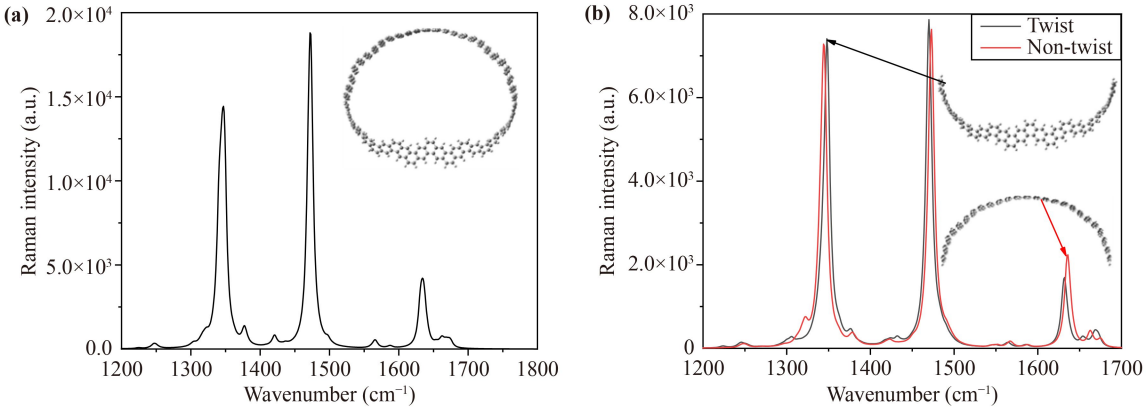

Fig. 7 Raman spectra of Möbius CNB and its twist and non-twist moieties. **(a)** Raman spectra of Möbius CNB, and **(b)** Raman spectra of twist and non-twist moieties, respectively.

being explored. In the future, Möbius CNBs may be used to study the catalysis application in 2D graphynes-based materials [32], and hydrogen evolution performance [33]. Also, Möbius CNBs may be coupled to transition metal dichalcogenides heterostructures or other 2D materials to provide optoelectrical properties [34–38]. Our work provides a deeper understanding of photophysical mechanisms of Möbius CNBs in one- and two-photon absorption and reveals possible applications on optoelectronic devices.

Acknowledgements This work was supported by the National Natural Science Foundation of China (Nos. 91436102, 11874407, and 11374353) and the Fundamental Research Funds for the Central Universities (No. 06500067).

References

1. Y. Segawa, T. Watanabe, K. Yamanoue, M. Kuwayama, K. Watanabe, J. Pirillo, Y. Hijikata, and K. Itami, Synthesis of a Möbius carbon nanobelt, *Nat. Synth.* 1(7), 535 (2022)
2. B. Yao, X. Liu, T. Guo, H. Sun, and W. Wang, Molecular Möbius strips: Twist for a bright future, *Org. Chem. Front.* 9(15), 4171 (2022)
3. A. Bedi and O. Gidron, The consequences of twisting nanocarbons: Lessons from tethered twisted acenes, *Acc. Chem. Res.* 52(9), 2482 (2019)
4. D. Ajami, O. Oeckler, A. Simon, and R. Herges, Synthesis of a Möbius aromatic hydrocarbon, *Nature* 426(6968), 819 (2003)
5. R. Kumar, H. Aggarwal, and A. Srivastava, Of twists and curves: Electronics, photophysics, and upcoming applications of non-planar conjugated organic molecules, *Chemistry* 26(47), 10653 (2020)
6. T. Bauer, P. Banzer, E. Karimi, S. Orlov, A. Rubano, L. Marrucci, E. Santamato, R. W. Boyd, and G. Leuchs, Observation of optical polarization of Möbius strips, *Science* 347(6225), 964 (2015)
7. M. Rickhaus, M. Mayor, and M. Juríček, Chirality in curved polyaromatic systems, *Chem. Soc. Rev.* 46(6), 1643 (2017)
8. G. Ouyang, L. Ji, Y. Jiang, F. Würthner, and M. Liu, Self-assembled Möbius strips with controlled helicity, *Nat. Commun.* 11(1), 5910 (2020)
9. J. F. Ayme, J. E. Beves, C. J. Campbell, and D. A. Leigh, Template synthesis of molecular knots, *Chem. Soc. Rev.* 42(4), 1700 (2013)
10. C. P. Collier, G. Mattersteig, E. W. Wong, Y. Luo, K. Beverly, J. Sampaio, F. M. Raymo, J. F. Stoddart, and J. R. Heath, A [2]catenane-based solid state electronically reconfigurable switch, *Science* 289(5482), 1172 (2000)
11. M. Stępień, L. Latos Grażyński, N. Sprutta, P. Chwalisz, and L. Szterenberg, Expanded porphyrin with a split personality: A Hückel–Möbius aromaticity switch, *Angew. Chem. Int. Ed.* 46(41), 7869 (2007)
12. J. Sankar, S. Mori, S. Saito, H. Rath, M. Suzuki, Y. Inokuma, H. Shinokubo, K. Suk Kim, Z. S. Yoon, J. Y. Shin, J. M. Lim, Y. Matsuzaki, O. Matsushita, A. Muranaka, N. Kobayashi, D. Kim, and A. Osuka, Unambiguous identification of Möbius aromaticity for meso-aryl-substituted [28]hexaphyrins(1.1. 1.1. 1.1), *J. Am. Chem. Soc.* 130(41), 13568 (2008)
13. Z. S. Yoon, A. Osuka, and D. Kim, Möbius aromaticity and antiaromaticity in expanded porphyrins, *Nat. Chem.* 1(2), 113 (2009)
14. G. R. Schaller, F. Topić, K. Rissanen, Y. Okamoto, J. Shen, and R. Herges, Design and synthesis of the first triply twisted Möbius annulene, *Nat. Chem.* 6(7), 608 (2014)
15. X. Jiang, J. D. Laffoon, D. Chen, S. Pérez Estrada, A. S. Danis, J. Rodríguez López, M. A. Garcia Garibay, J. Zhu, and J. S. Moore, Kinetic control in the synthesis of a Möbius tris((ethynyl)[5]helicene) macrocycle using alkyne metathesis, *J. Am. Chem. Soc.* 142(14), 6493 (2020)
16. D. M. Walba, R. M. Richards, and R. C. Haltiwanger, Total synthesis of the first molecular Möbius strip, *J. Am. Chem. Soc.* 104(11), 3219 (1982)
17. Q. H. Guo and J. F. Stoddart, The making of aromatic molecular Möbius belts, *Chem* 8(8), 2076 (2022)
18. T. W. Price and R. Jasti, Carbon nanobelts do the twist, *Nat. Synth.* 1, 502 (2022)
19. Y. Chen, Y. Cheng, and M. Sun, Physical mechanisms on plasmon-enhanced organic solar cells, *J. Phys. Chem. C* 125(38), 21301 (2021)
20. Y. Chen, Y. Cheng, and M. Sun, Nonlinear plexcitons: Excitons coupled with plasmons in two-photon absorption, *Nanoscale* 14(19), 7269 (2022)
21. W. Kohn and L. J. Sham, Self-consistent equations including exchange and correlation effects, *Phys. Rev.* 140(4A), A1133 (1965)
22. A. Becke, Density-functional thermochemistry (iii): The role of exact exchange, *J. Chem. Phys.* 98(7), 5648 (1993)
23. C. Lee, W. Yang, and R. G. Parr, Development of the Colle-Salvetti correlation-energy formula into a functional of the electron density, *Phys. Rev. B* 37(2), 785 (1988)
24. M. Frisch, G. Trucks, H. Schlegel, G. Scuseria, M. Robb, J. Cheeseman, G. Scalmani, V. Barone, G. Petersson, and H. Nakatsuji, Gaussian 16, Revision C. 01, Gaussian, Inc. , Wallingford Ct. , 2020
25. E. Gross and W. Kohn, Local density-functional theory of frequency-dependent linear response, *Phys. Rev. Lett.* 55(26), 2850 (1985)
26. T. Yanai, D. P. Tew, and N. C. Handy, A new hybrid exchange–correlation functional using the Coulomb-attenuating method (Cam-B3lyp), *Chem. Phys. Lett.* 393(1–3), 51 (2004)
27. T. Lu and F. Chen, Multiwfn: A multifunctional wavefunction analyzer, *J. Comput. Chem.* 33(5), 580 (2012)
28. Z. Liu, T. Lu, and Q. Chen, An sp-hybridized all-carboatomic ring, cyclo[18]carbon: Electronic structure, electronic spectrum, and optical nonlinearity, *Carbon* 165, 461 (2020)
29. M. Göppert-Mayer, Über elementarakte mit zwei quantensprüngen, *Ann. Phys.* 401(3), 273 (1931)
30. S. Kraner, R. Scholz, F. Plasser, C. Koerner, and K. Leo, Exciton size and binding energy limitations in one-dimensional organic materials, *J. Chem. Phys.* 143(24),

244905 (2015)
31. S. Mukamel, S. Tretiak, T. Wagersreiter, and V. Chernyak, Electronic coherence and collective optical excitations of conjugated molecules, *Science* 277(5327), 781 (1997)
32. N. Zhang, J. Wu, T. Yu, J. Lv, H. Liu, and X. Xu, Theory, preparation, properties and catalysis application in 2D graphynes-based materials, *Front. Phys.* 16(2), 23201 (2021)
33. Q. Kong, X. An, L. Huang, X. Wang, W. Feng, S. Qiu, Q. Wang, and C. Sun, A DFT study of $Ti_3C_2O_2$ MXenes quantum dots supported on single layer graphene: Electronic structure an hydrogen evolution performance, *Front. Phys.* 16(5), 53506 (2021)
34. R. Yang, J. Fan, and M. Sun, Transition metal dichalcogenides (TMDCs) heterostructures: Optoelectric properties, *Front. Phys.* 17(4), 43202 (2022)
35. X. H. Li, Y. X. Guo, Y. Ren, J. J. Peng, J. S. Liu, C. Wang, and H. Zhang, Narrow-bandgap materials for optoelectronics applications, *Front. Phys.* 17(1), 13304 (2022)
36. Z. B. Dai, G. Cen, Z. Zhang, X. Lv, K. Liu, and Z. Li, Near-field infrared response of graphene on copper substrate, *Front. Phys.* 17(4), 43502 (2022)
37. G. Luo, X. Lv, L. Wen, Z. Li, and Z. Dai, Strain induced topological transitions in twisted double bilayer graphene, *Front. Phys.* 17(2), 23502 (2022)
38. S. Y. Li and L. He, Recent progresses of quantum confinement in graphene quantum dots, *Front. Phys.* 17(3), 33201 (2022)